Microphthalmia-associated Transcription Factor Regulates *RAB27A* Gene Expression and Controls Melanosome Transport[*]

Christine Chiaverini[‡§¶1], **Laurent Beuret**[‡§2], **Enrica Flori**[||], **Roser Busca**[‡3], **Patricia Abbe**[‡§], **Karine Bille**[‡§], **Philippe Bahadoran**[‡§¶], **Jean-Paul Ortonne**[‡§¶], **Corine Bertolotto**[‡§¶], and **Robert Ballotti**[‡§¶4]

From the ‡*INSERM U895, Biologie et Pathologies des Cellules Mélanocytaires de la Pigmentation Cutanée au Mélanome 28, avenue de Valombrose, 06107 Nice Cedex 2, France, the* §*Université de Nice Sophia-Antipolis, UFR Médecine, Nice, F-06107, France, the* ¶*CHU Nice, Department of Dermatology, 152, route de Saint Antoine de Ginestière, 06200 Nice, France, and* ||*Laboratorio di Fisiopatologia Cutanea, Istituto Dermatologico San Gallicano, IRCCS, 00153-Roma, Italy*

Melanosomes are lysosome-related organelles specialized in melanin synthesis and transport. In this study, we show that microphthalmia-associated transcription factor (MITF) silencing induces melanosome gathering around the nucleus and causes the relocalization of Rab27A, Slac2a-Mlph, and Myo5a that control the transport of melanosomes on the actin network. In an attempt to elucidate the mechanism by which MITF controls melanosome distribution, we identify *RAB27A* as a new MITF target gene. Indeed, MITF silencing leads to a dramatic decrease in Rab27A expression and blocks the stimulation of Rab27A expression evoked by cAMP. Further, forced expression of MITF increases Rab27A expression, indicating that MITF is required and sufficient for Rab27A expression in melanoma cells. MITF binds to two E-boxes in the proximal region of the Rab27A promoter and stimulates its transcriptional activity. Finally, re-expression of Rab27A, in MITF-depleted cells, restores the transport of melanosomes to the cell periphery. These results show that *RAB27A* is a new direct transcriptional target of MITF and link MITF to melanosome transport, another key parameter of melanocyte differentiation and skin pigmentation. Interestingly, Rab27A is involved in other fundamental physiological functions, such as the transport of lytic granules and insulin secretion. Thus our results, deciphering the mechanism of Rab27A transcriptional regulation, have an interest that goes beyond the skin pigmentation field.

In humans, pigmentation results from the synthesis and distribution of melanin in skin, hair bulbs, and eyes (1). Melanin synthesis or melanogenesis is an enzymatic process, catalyzed by tyrosinase, Tyrp1 (tyrosinase-related protein 1), and dopachrome tautomerase (DCT),[5] which converts tyrosine to melanin pigments. This process takes place in melanocytes within lysosome-related vesicles named melanosomes that are transported to the dendrites tips and transferred to surrounding keratinocytes to ensure hair and skin pigmentation. In humans, melanins play a key photo-protective role against the noxious effect of UV radiation from solar light.

Numerous studies have been undertaken to understand the molecular mechanisms that control melanosome distribution within melanocytes. It has been demonstrated that melanosomes are subjected to both a bidirectional microtubule-dependent transport and an unidirectional actin-dependent transport that allow melanosome docking at the dendrite tips (2).

The microtubule-dependent transport of melanosomes is controlled by kinesin for transport toward the cell periphery, whereas the minus-end motility toward the cell center is mediated by dynein that is linked to melanosome by the Rab7-RILP (Rab7-interacting lysosomal protein) complex (3). At the cell periphery, the Rab27A-melanophilin (Slac2a-Mlph) complex recruits the actin-dependent motor protein, myosin 5a (Myo5a), allowing melanosomes to move on the actin network (4–6).

The following step is the anchoring of melanosomes to the plasma membrane through simultaneous interaction of Slp2, with Rab27A on the melanosomes and phosphatidylserine at the plasma membrane (7).

In humans, α-melanocyte-stimulating hormone is a key physiological regulator of melanocyte differentiation and skin pigmentation (8). α-Melanocyte-stimulating hormone binds to the melanocortin receptor type 1 and activates the cAMP pathway, thereby leading to a stimulation of melanogenesis (9). Recently we have demonstrated that cAMP rapidly increases the interaction of the Slac2a-Mlph with actin and leads to the rapid accumulation of melanosomes in the actin-rich region of the dendrite extremities. Further, cAMP stimulates the expression of Rab27A that could facilitate the interaction of melanosomes with cortical actin (10).

In melanocytes the effects of cAMP on melanin synthesis are mediated by microphthalmia-associated transcription factor (MITF), which is the master gene of melanocyte development,

---

differentiation, and survival. Until now MITF has been demonstrated to control the expression of tyrosinase, Tyrp1, and DCT, the enzymes that are essential for melanin production (11, 12). MITF also controls genes involved in melanosome genesis or structure such as *MART1*, *Silver*, and *GPR143 (OA1)* (13). The gene encoding the melanosomal protein, TRPM1, with unknown function is also a MITF target gene (13). However, until now MITF has never been involved in the regulation of melanosome transport. In this study we have dissected the regulation of melanosome transport by MITF in human and mouse melanoma cells. We demonstrate that MITF regulates the peripheral distribution of melanosomes to the dendrite tips via the control of Rab27A expression. MITF directly binds to the Rab27A promoter, thereby increasing its activity. Re-expression of Rab27A in MITF-depleted B16 cells restores the peripheral melanosome transport. Taken together, we demonstrate the involvement of MITF in the actin-dependent melanosome transport that is, together with melanin synthesis, a key functional trait of differentiated melanocytes underlying skin pigmentation.

MATERIALS AND METHODS

Cell Culture, Transfection, and Infection—Mouse melanoma B16-F10 cells, human melanoma Mel501 cells, and A375 cells were cultured in Dulbecco's modified Eagle's medium supplemented with 7% fetal bovine serum and penicillin/streptomycin (100 IU; 50 μg/ml) in a humidified atmosphere containing 5% CO_2 at 37 °C. B16 and Mel501 cells were transfected with Lipofectamine (Invitrogen) according to the protocol of the manufacturer. In brief, 3×10^6 cells in 100-cm^2 culture dishes were transfected with 70 μl of Lipofectamine and 15 μg of plasmid or 100 nM of siRNAs in Optimen. After 6 h, the cells were replaced in Dulbecco's modified Eagle's medium supplemented with 7% fetal bovine serum. A375 cells were infected with control and MITF encoding adenovirus for 72 h as described elsewhere (11).

Plasmid, siRNA, and Adenovirus—Rab27A-GFP and GFP-N1 plasmids were described previously (4). siRNA-mediated down-regulation of MITF was achieved with a specific MITF siRNA (36), and scrambled siRNA was used as control. Recombinant adenovirus encoding wild type MITF (Ad-MITF) was previously described (11).

Antibodies—A polyclonal anti-melanophilin antibody was obtained by immunization of rabbits with two peptides within the C-terminal domain of mouse melanophilin and was used at 1/500 dilution for Western blot (WB) and 1/50 dilution for immunofluorescence (IF) (10). Polyclonal antibody to Tyrp1 (PEP1) (from Dr. Hearing, NCI, National Institutes of Health) were used at 1/2,000 dilution for WB and 1/200 for IF. Monoclonal antibodies to Tyrp1 (B8G3) (from Dr Parson) and to Silver protein (HMB45) (Dakopatts) were used respectively at 1/15 and 1/100 dilution for IF. Monoclonal antibody to MITF (C5) (Abcam) was used at 1/100 dilution for WB and 1/10 for IF. Polyclonal antibody to the C terminus part of MITF, used at 1/250, was previously described (37). The monoclonal antibody to Rab27A (Transduction Laboratories), and the polyclonal antibody to Myo5a (provided by Dr. Mooseker, Yale University, New Haven, CT) were used at 1/2000 for WB and 1/100 for IF.

The monoclonal ERK2 antibody (Santa Cruz Biotechnology) was used at 1/2000 for WB. The anti-mouse and anti-rabbit peroxidase-conjugated secondary antibodies as well as the fluorescein isothiocyanate and Texas Red-conjugated anti-mouse and anti-rabbit antibodies were from Dakopatts.

Immunofluorescence Study—B16 or Mel501 cells cultured on glass coverslips were washed three times in PBS, fixed for 20 min in 3% paraformaldehyde, washed again, and incubated for 10 min in 50 mM NH_4Cl after three more PBS washes. The cells were next incubated with the primary antibody diluted in PBS containing 0.5% bovine serum albumin and 0.02% saponin for 1 h, washed abundantly in PBS, and incubated for another hour with the appropriate conjugated secondary antibody. After washing, the coverslips were mounted on glass slides and viewed with an Axiophot fluorescent microscope (Zeiss).

Western Blot—Proteins 40 μg were separated on SDS-PAGE and transferred onto polyvinylidene difluoride membranes. The membranes were saturated in a saline buffer, 2% bovine serum albumin and then incubated with the corresponding primary antibody for 1 h at room temperature. After three 10-min washes in a saline buffer containing 0.05% Triton X-100, the blots were incubated for 1 h with the corresponding peroxidase-conjugated secondary antibody and washed again. The antigen-antibody complex was detected with the ECL kit (Amersham Biosciences).

Construction of the Reporter Plasmids—A 800-bp fragment 5' of the transcriptional start site of the Rab27A transcript was isolated and amplified by PCR and then inserted into plasmid vector pCR2.1-TOPO (TOPO TA Cloning®, Invitrogen). The 800-bp fragment was subcloned into the unique XhoI and SacI restriction site of the pGL3basic vector (pGL3B), upstream of the luciferase coding sequence (pR27a). The first nucleotide of the first exon was numbered 1. For the deletion constructs, pR27a was cut with EcoRV (0.6 kb) or BsgI (0.2 kb) and then self-ligated with T4 DNA ligase, giving, respectively, the following plasmids: pR27a-Δ1 and pR27a-Δ2. pR27A-mE1, pR27A-mE2, and pR27A-mE3 mutants were constructed with the Transformer™ site-directed mutagenesis kit (Clontech Laboratories, Inc., Palo Alto, CA). Briefly, the CANNTG sequence of each E-box was replaced by a TCNNTG sequence using the following oligonucleotide: E-box 1 (5'-GAAAGGGGCAAAAATT-CCTTGACTGGTCTGCAGTGCC-3'), E-box 2 (5'-ACTGGT-CTGCAGTGCTCTATGACAAACAGCTGAGAC-3'). The plasmid containing the MITF coding sequence in pCDNA3 was previously described (38).

Luciferase Assays—B16 melanoma cells were seeded in 24-well dishes, and transient transfections were performed the following day using 2 μl of Lipofectamine (Invitrogen) and 0.5 μg of total plasmid DNA in a 200-μl final volume. pCMV-βGal was cotransfected with the tested plasmids to control transfection efficiency. 24 h after transfection, soluble extracts were harvested in 50 μl of lysis buffer and assayed for luciferase and β-galactosidase activities. All of the transfections were repeated at least five times using different plasmid preparations.

Gel Mobility Shift Assay—Double-stranded synthetic E1 box (5'-TATGACAAACAGCTGAGAC-3'), E2-box (5'-CTGCA-GTGCCATATGACAAACAGC-3') and corresponding mutated boxes, mE1 and mE2 (5'-TATGACAAATCGCTGA-
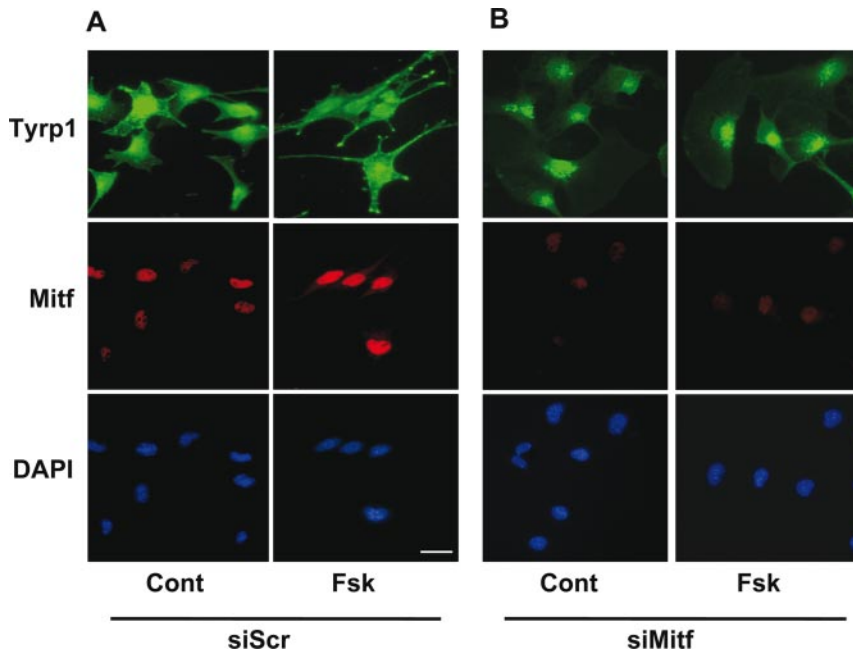
FIGURE 1. **Mitf silencing blocks the peripheral melanosomal transport.** B16 melanoma cells were transfected with siScr (*A*) or siMITF (*B*) and exposed to forskolin (20 μM) for 24 h. Melanosomes were labeled with a polyclonal antibody to Tyrp1 (pep1). Mitf was labeled with the monoclonal antibody C5. A mouse anti-rabbit fluorescein isothiocyanate (1/1000) and a goat anti-mouse Texas Red (1/600) were used as secondary antibodies. *Bar*, 20 μm. The nuclei were stained with 4′,6′-diamino-2-phenylindole (*DAPI*). Three independent experiments were performed. The images are representative of >85% of cells of 150 cells analyzed in each condition. *Cont*, control.

GAC-3′ and 5′-CTGCAGTGCTCTATGACAAACAGC-3′) were end-labeled with [γ-^{32}P]ATP (Amersham Biosciences) and T4 polynucleotide kinase. Nuclear extracts from B16 cells, prepared as previously described (12), were preincubated in binding buffer for 15 min on ice. Then 30,000–50,000 cpm of ^{32}P-labeled probe were added to the binding reaction for 10 min at room temperature. DNA-protein complexes were resolved by electrophoresis on 4% polyacrylamide gel (37.5:1;acrylamide/bisacrylamide) in TBE buffer (22.5 mM Tris borate, 0.5 mM EDTA, pH 8) for 2 h at 150 V.

Chromatin Immunoprecipitation Assay—B16 cells were cultured in 100-cm^2 culture dishes, stimulated (or not) with forskolin for 5 h, and then treated with 1% formaldehyde for 10 min at 37 °C. Next, the cells were harvested in PBS, centrifuged (700 $\times$ *g*, 5 min at 4 °C), and suspended in the lysis buffer (EZ ChIP^{TM} chromatin immunoprecipitation kit; Upstate). After sonication the sheared chromatin was then immunoprecipitated using indicated antibodies. After immunoprecipitation, the cross-link was reverted by heat treatment (65 °C overnight and proteinase K digestion). The genomic captured fragments were purified using spin columns. Identification of the captured DNA fragments was performed by PCR analysis using the Rab27A or GAPDH promoter primers. 30 cycles of PCR were performed, and the amplified products were analyzed on a 2% agarose gel.

RESULTS

Mitf Silencing Affects Melanosome Distribution in B16 Melanoma Cells—In B16F10 melanoma cells, immunofluorescence labeling with antibody to Tyrp1 (Fig. 1, *green*) showed that
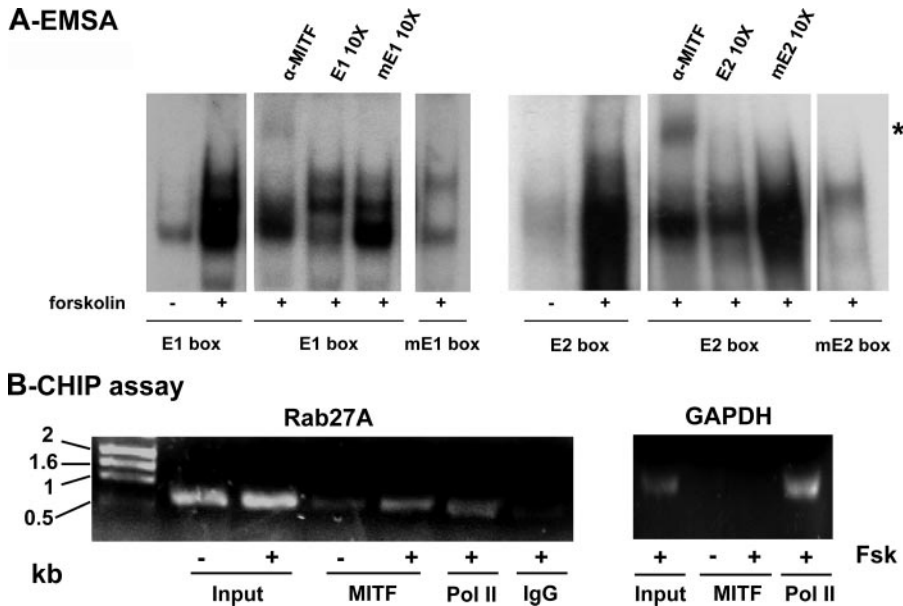
melanosomes were distributed all over the cells. After forskolin treatment for 24 h, we observed that cells acquired a dendritic phenotype and that melanosomes were gathered at the dendrite tips. We also observed an increased Mitf expression after forskolin treatment (Fig. 1*A*). These observations prompted us to hypothesize that Mitf might play a role in the control of melanosome distribution. Indeed, transfection with specific *Mitf* siRNA dramatically inhibited Mitf expression, in both basal and forskolin conditions, in more than 98% of the cells. Interestingly, Mitf silencing altered melanosome distribution and prevented melanosome docking at dendrite tips in forskolin-treated cells (Fig. 1*B*). These observations indicate that Mitf is involved in the cAMP regulation of melanosome peripheral distribution.

Mitf Silencing Induces Relocalization of the Myosin 5a, Slac2a-Mlph, Rab27A, and Inhibits Rab27A Expression—Peripheral melanosome transport involves a tripartite complex composed of Myo5a, Slac2a-Mlph, and Rab27A that allows melanosomes to interact and move on actin filament. Hence, we studied the effect of Mitf silencing on these proteins. B16 melanoma cells were transfected with scrambled or *Mitf* siRNA (siMITF) and then exposed for 24 h to forskolin. Mitf and Myo5a, Slac2a-Mlph, or Rab27A expression was analyzed by immunofluorescence. In cells transfected with scrambled siRNA (siScr), Myo5a, Slac2a-Mlph and Rab27A all showed a reinforced localization at the cell periphery, whereas after Mitf silencing as shown by the absence of red labeling, these proteins were relocalized within the cell body (Fig. 2*A*). Therefore Mitf silencing impairs Myo5a-Mlph-Rab27A tripartite complex distribution.

Next, we hypothesize that Mitf might control the expression of one or several members of the tripartite complex that allow melanosome peripheral distribution. To verify this hypothesis, B16 melanoma cells were transfected with scrambled or Mitf siRNA and treated or not with forskolin. Myo5a, Slac2a-Mlph, Rab27A protein expression was analyzed by Western blot (Fig. 2*B*). In control conditions, forskolin increased Mitf, tyrosinase, Myo5a, and Rab27A expression. Slac2a-Mlph expression was not affected by forskolin. Transfection with siMITF dramatically reduced Mitf expression. In these cells, we observed an almost complete extinction of tyrosinase and Rab27A expression. Slac2a-Mlph or ERK2 expression was not affected compared with cells transfected with scrambled siRNA. A slight, but reproducible decrease (15–25%) in Myo5a expression was also observed.

FIGURE 2. **Mitf silencing relocalizes the proteins involved in actin-dependent melanosomal transport and controls Rab27A expression.** *A*, B16 melanoma cells were transfected with siScr or siMITF (100 nmol) and exposed to forskolin (20 μM) for 24 h. The cells were labeled with a polyclonal antibody to Myo5a or melanophilin and with a mouse monoclonal antibody to Mitf (C5). When cells were labeled with a monoclonal antibody to Rab27A, Mitf was visualized with a polyclonal antibody to Mitf. *Bar*, 10 μm. Three independent experiments were performed. The images are representative of >85% of cells of 150 cells analyzed in each condition. *B*, B16 melanoma cells were transfected with siScr or siMITF and exposed or not to forskolin (20 μM) for 24 h. WB analysis was performed using polyclonal antibodies to Myo5a, melanophilin, tyrosinase, and monoclonal antibodies to Rab27A, Mitf, and ERK2.

Mitf Stimulates Rab27A Transcription and Binds Directly to the Rab27A Promoter—Next, we analyzed the effect of Mitf silencing on Rab27A messengers. Real time PCR analysis showed that forskolin treatment increased the mRNA levels of Mitf, tyrosinase, and Rab27A. On the other hand, in cells transfected with siMITF, we observed a dramatic decrease in Mitf, tyrosinase, and Rab27A messengers (Fig. 3*A*), suggesting that Mitf controlled Rab27A expression at the transcriptional level. To perform a functional analysis of the Rab27A promoter, we cloned a 800-bp fragment of the *Rab27A* gene from +33 to −870 according to Tolmachova *et al.* (14) upstream from the luciferase reporter gene. This fragment contains seven E-boxes susceptible to

FIGURE 3. **Mitf stimulates Rab27A transcription and stimulates the Rab27A promoter activity.** *A*, B16 melanoma cells melanoma cells were transfected with siScr or siMITF and exposed or not to forskolin (20 μM) for 24 h. RNA were purified and relative amounts of Mitf, Rab27A, and tyrosinase messengers were quantified by real time quantitative PCR. *B*, schematic representation of the Rab27A promoter containing seven E-boxes (*E1–E7*). The *black arrows* denote the sites of restriction enzymes EcoRV and BsgI used for R27a-Δ1 and R27a-Δ2 constructs, respectively. The *white arrow* denotes the initiation of the transcription. *C*, alignment of human and mouse RAB27A promoter was performed using BLAST program (NCBI). Exon 1 of the human RAB27A gene is shown in *bold type*. *D*, B16 cells were transfected in Lipofectamine with 0.3 μg of pR27a-wt, pR27a-Δ1, pR27a-Δ2, pR27a-mE1, pR27a-mE2, pR27a-mE3, and 0.05 μg of pCMVβGAL and 0.2 μg of pMITF or not. After 24 h with forskolin, luciferase activity was normalized by the β-galactosidase activity, and the results were expressed as fold stimulation of the basal luciferase activity of nonstimulated cells. The data are the means ± S.E. of five experiments performed in triplicate.

FIGURE 4. **Mitf binds to the two proximal E-boxes of the Rab27A promoter.** *A*, gel shift experiments were performed with B16 nuclear extracts from control or forskolin treated cells, using labeled wild type (E1 or E2 box) or mutated (mE1 box, mE2 box) probes. When indicated, the reactions were carried out in presence of an excess (10-fold) of unlabeled homologous or mutated probe or with 2.5 μg of anti-Mitf antibody. The *asterisk* indicates the complexes supershifted by the Mitf antibody. *B*, chromatin immunoprecipitations were performed on extracts from nonstimulated and forskolin-stimulated (*Fsk*) B16 melanoma cells. Immunoprecipitation was performed using specific anti-Mitf, anti-polymerase II (*Pol II*) antibodies, and rabbit IgG (IgG) as control. Primers spanning the Rab27A promoter region were used for the PCR amplification. A control of PCR amplification was performed on nonimmunoprecipitated extracts (*Input*). Another control was performed using a primer pair to the human GAPDH promoter.

bind Mitf (Fig. 3*B*). Further, human and mouse Rab27A promoters show a strong homology in the proximal region. This region contains three E-boxes that are conserved in both mouse and human promoters (Fig. 3*C*). Functional analysis of this promoter fragment (Fig. 3*D*) showed that the Rab27A promoter was responsive to cAMP, because forskolin treatment led to a 5-fold increase in the luciferase activity. Cotransfection of the Rab27A promoter reporter construct with an expression plasmid encoding Mitf also strongly increased the promoter activity. Taken together, these data demonstrate that Mitf regulates Rab27A expression at the transcriptional level.

Then we studied two deletion constructs that removed one (pR27a-D1) and four E-boxes, respectively (pR27a-D2), at the 5′ end of the promoter. Both constructs showed almost the same responsiveness to cAMP and Mitf compared with the wild type construct. These data indicate that the cAMP- and Mitf-responsive elements are located within proximal region containing three E-boxes. Individual mutation of these E-boxes showed that mutation of the most 5′ E-box (E-box3) did not affect the stimulation of the Rab27A promoter activity by cAMP or Mitf, whereas mutation of either E-box 1 or E-box 2 led to a strong decrease in the stimulation elicited by cAMP or by Mitf. Thus E-boxes 1 and 2 likely bind Mitf and mediate the effect of cAMP.

To verify that Mitf indeed binds to the Rab27A promoter, we performed a gel shift assay with labeled E-boxes 1 and 2. Nuclear extracts from B16 melanoma cells exposed to forskolin showed an increased binding to the labeled E-box 1 and 2 (Fig. 4). In each case, the binding was displaced by an excess of the unlabeled probe but not or slightly affected by an excess of

unlabeled mutated corresponding E-box. Mitf was identified as the protein that binds to the E-box 1 and 2, because an anti-Mitf antibody dramatically reduced the formation of the complexes with E-box 1 and 2 and induced a weak supershift of the complexes.

To verify the binding of Mitf to the Rab27A promoter in intact cells, we performed a chromatin immunoprecipitation assay in B16 melanoma cells. Direct PCR amplification, with specific primers spanning the Rab27A promoter, on crosslinked protein-DNA total extract amplified a band of 800 bp (Fig. 4*B*, *left panel*, *Input*). Alternatively, the extracts were first immunoprecipitated with antibody to polymerase II as positive control, nonimmune rabbit IgG as a negative control or anti-Mitf antibody. After immunoprecipitation with anti-Mitf, we amplified a band at 800 bp corresponding to the Rab27A promoter. This band was clearly increased in extracts from cells exposed to forskolin. We also amplified the Rab27A promoter in anti-Pol II precipitates, but not in nonimmune antibody precipitates. Instead, using PCR amplification with specific GAPDH promoter primers, we amplified a 1-kb fragment corresponding to the GAPDH promoter both in the total input and in the anti-Pol II precipitates, but not in the anti-Mitf precipitates (Fig. 4*B*). These results demonstrate that Mitf binds to the Rab27A promoter in intact cells.

Rab27A Re-expression Restores Normal Melanosome Distribution in Mitf-deficient Melanoma Cells—We wished to assess whether the loss of Rab27A expression in Mitf-deficient cells was indeed responsible for the aberrant distribution of melanosomes. In this aim, we expressed Rab27A-GFP in B16 melanoma cells transfected with siMITF (Fig. 5). As previously observed, Mitf silencing induced melanosome (visualized with an anti-Tyrp1 antibody, red) gathering at the cell center, compared with cell transfected with scrambled siRNA. However, in the cells that expressed Rab27A-GFP (Fig. 5, *green*), melanosomes spread all over the cells and reached the dendrite tips. This observation was made in more than 90% of the cell lacking Mitf and that re-expressed Rab27A. In contrast, in cells that expressed GFP alone, melanosome distribution was not modified compared with nontransfected cells. Therefore forced Rab27A expression is able to restore melanosome peripheral distribution in Mitf-depleted cells.

MITF Controls RAB27A Expression and Melanosome Distribution in Human Melanoma Cells—Finally, we wished to confirm that MITF also controlled melanosome distribution in human cells. We performed the same experiment in human melanoma cells Mel501, and we observed, as is the case in B16
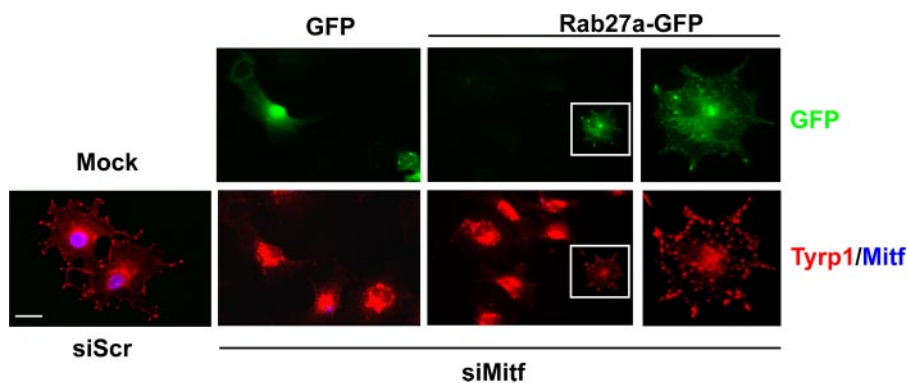
FIGURE 5. Rab27A re-expression relocalizes melanosomes to the tips of dendrites in Mitf-silenced B16 melanoma cells. B16 cells were transfected with siMITF and Rab27a-GFP or GFP alone 24 h later and then exposed to forskolin (20 μM) for 24 h. the melanosomes were visualized with polyclonal antibody to Tyrp1 (pep1) and secondary antibody-labeled with Texas Red. Mitf was visualized with the monoclonal antibody C5 and Alexa fluor 350 anti-mouse antibody. *Bar*, 10 μm. Three independent experiments were performed. The images are representative of >85% of cells of 30 cells analyzed in each condition.
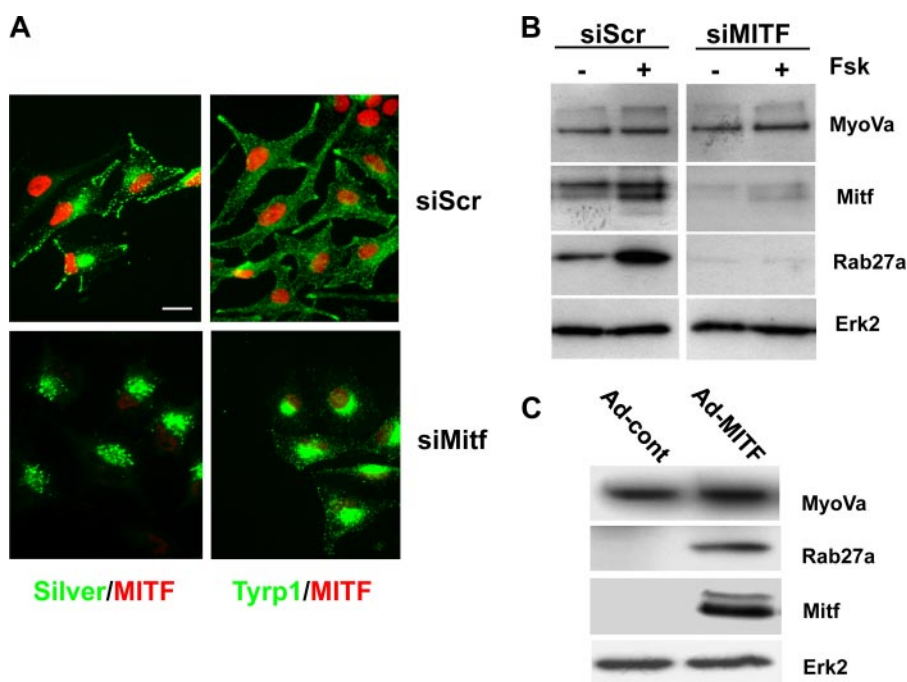
FIGURE 6. MITF controls RAB27A expression and melanosome distribution in human melanoma cells. *A*, Mel501 melanoma cells were transfected with siScr or siMITF and then exposed to forskolin (20 μM) for 24 h. the melanosomes were labeled with monoclonal antibodies to Trp1 (B8G3) and Silver (HMB45). MITF was labeled with polyclonal antibody to the C-terminal part of the protein. *Bar*, 10 μm. Three independent experiments were performed. The images are representative of >85% of cells of 150 cells analyzed in each condition. *B*, Mel501 melanoma cells were transfected with siScr or siMITF and exposed or not to forskolin (20 μM) for 24 h. WB analysis was performed using polyclonal antibodies to Myo5a and monoclonal antibodies to Rab27a, MITF, and ERK2. *C*, A375 melanoma cells were infected with control adenovirus (*Ad-cont*) or adenovirus expressing MITF (*Ad-MITF*) for 72 h. WB analysis was performed using a polyclonal antibody to Myo5a and monoclonal antibodies to Rab27a, MITF (C5), and ERK2.

melanoma cells, that MITF silencing led to striking melanosome gathering at the cell center compared with cells expressing MITF (Fig. 6*A*). Western blot analysis confirmed that siMITF dramatically inhibited both MITF and RAB27A expression but did not affect MYO5A level (Fig. 6*B*). Thus MITF appears to be required for RAB27A expression.

To investigate whether MITF was sufficient to trigger RAB27A expression, we infected A375 human melanoma cells, which express a very low level of MITF, with an empty adenovirus or an adenovirus encoding wild type MITF. We observed

that infection with MITF-encoding adenovirus led to a strong increase in both MITF and RAB27A expression (Fig. 6*C*), whereas the empty adenovirus did not affect the level of RAB27A protein. Forced MITF expression did not affect MYO5A expression. Identical results have been obtained in SKmel28 human melanoma cells. Taken together, our data demonstrate that MITF is required and sufficient for RAB27A expression in human melanoma cells.

DISCUSSION

In the present report, we identify *RAB27A* as a new MITF target gene and show the involvement of MITF in melanosome distribution within melanoma cells. Indeed, MITF silencing induces melanosome gathering around the nucleus and leads to a dramatic decrease in Rab27A expression. In both mouse and human melanoma cells, cAMP elevating agents increase Rab27A expression. This effect is blocked by MITF silencing, indicating that MITF mediates the effects of cAMP on Rab27A expression. Further, adenovirus-forced expression of MITF increases Rab27A protein level, demonstrating that MITF is sufficient to trigger Rab27A expression. Conversely, tyrosinase, which is also a MITF target gene, is not induced by ectopic expression of MITF (11). Tyrosinase gene appears to have a nonpermissive chromatin conformation, and MITF needs to recruit the SWI/SNF complex that allow chromatin remodeling and tyrosinase expression (15). *RAB27A*, as well *HIF1A* (16), *BCL2* (17), and *MET* (18, 19), which do not require SWI/SNF complex to be regulated by MITF, appear to be in an active genomic region.

In our study, melanosomes are visualized by Tyrp1 or Silver labeling. Indeed, in cells transfected with siMITF, it is not possible to observe black melanosomes containing melanin, because MITF silencing causes a complete and rapid loss of tyrosinase and melanin content in pigmented melanoma cells. Thus we cannot rule out the possibility that MITF silencing affects Tyrp1 and Silver targeting to melanosomes. However, MITF silencing obviously affects the distribution of both Tyrp1 and Silver containing vesicles.

Rab27A has been reported to stabilize MLPH (20). Thus the loss of rab27 in MITF-silenced cells was expected to decrease MLPH expression. However, in our experiments the level of MLPH is not affected by MITF silencing. This observation might be explained by a residual amount of Rab27A that is sufficient to stabilize MLPH but not to ensure a correct melanosome transport. Several other RAB proteins, including RAB3A (21), RAB7 (3), and RAB8 (22, 23) have been involved in melanosome transport. However, in our hands, none of them are regulated by MITF (data not shown).

It is noteworthy that we observe that MITF silencing also induces morphologic changes in melanoma cells with a loss of the dendritic processes. Kuroda and Fukuda (7) reported that Slac2a-Mlph, a Rab27A effector, is required for elongated melanocyte shape, but this effect is independent of the ability of Slac2a-Mlph to bind Rab27A. Further, no morphology changes have been reported either in melanocyte from ashen mice (24) or in melanoma cells transfected with dominant negative form of Rab27A (25, 26). Thus the loss of Rab27A expression does not seem to be responsible for the cell shape modification. The effect of MITF silencing on melanoma cell shape might be explained by the inhibition of other MITF targets. A good candidate could be Diaph1, a new MITF target gene (27) that controls the actin cytoskeleton and cell morphology. Because the actin cytoskeleton plays a key role in melanosome transport, one could argue that changes in melanosome repartition might be the consequence of the alteration of the actin network. However, the inhibition of ROCK by Y27632, in cells depleted in MITF by specific siRNA restores dendricity but not peripheral melanosome localization (data not shown). Moreover, in MITF-depleted cells, re-expression of Rab27A restores melanosome transport to the cell periphery, demonstrating that the loss of Rab27A expression was the primary cause of melanosome mislocalization.

Within human and mouse *RAB27A* gene, we identify a promoter region at 5′ of the human transcript (NM 004580) that shows a strong homology with the 5′ region of the mouse transcript (AF 304376) described by Wilson *et al.* (24). Interestingly, within these regions, three proximal E-boxes are perfectly conserved. The functional analysis of the Rab27A promoter shows that this fragment is responsive to cAMP and MITF. Two more proximal E-boxes bind MITF and mediate the cAMP effect. Interestingly, the antibody to Mitf does not completely competed out the complexes formed with E1 and E2 probes, suggesting that other basic helix-loop-helix transcription factors such as TFE3 or USF1 can bind to these sequences, at least *in vitro*.

The sequences of these E-boxes (CATATG and CAGCTG) do not match perfectly with the consensus sequence (CATGTG) targeted by MITF in the other differentiation gene such as *TYR*, *TYRP1*, and *DCT* (28). However, recently several new MITF target genes (*CDKN1A*, *CDKN2A*, *CDK2*, *HIF1A*, and *BCL2*) (16, 17, 27, 29, 30) have been described, and the E-boxes targeted by MITF in these genes do not have the CATGTG canonical sequence.

In addition to melanosome transport, Rab27A has been involved in other biological functions such as secretion of cytotoxic granules by cytotoxic T lymphocyte (31) and insulin secretion by pancreas β cells (32). Interestingly, TFE3 and TFEB, which share a strong homology with MITF, are expressed in T lymphocyte (33). In these cells, TFE3 and TFEB might regulate Rab27A expression and thus the cytotoxic response. Similarly, NeuroD1/BETA2 is a key transcription factor required for pancreas endocrine cell differentiation. NeuroD1 is a basic helix-loop-helix transcription factor and binds to the E-box motif (34). Thus NeuroD1 might regulate insulin secretion through the control of Rab27A expression in pancreas β cells. In other cell types expressing Rab27A, the transcriptional regulation of this gene might involve a ubiquitous helix-loop-helix transcription factor such as Usf1 or Myc that could bind to the E-boxes of the Rab27A promoter.

Patients with Griscelli syndrome type 2 have hypopigmentation (skin and hairs) and a hemophagocytic syndrome caused by Rab27A mutation (35). However, some patients with these symptoms have no mutation in the Rab27A coding sequence. These cases might be explained by a reduced Rab27A expression, ensuing mutations in the E-boxes that bind MITF (or other basic helix-loop-helix transcription factors). Until now, we have sequenced the promoter region of five patients with Griscelli syndrome type 2 without mutation in Rab27A coding sequence. We found no mutation in the *RAB27A* promoter region of these patients.

In skin, UV radiations induce an increase of MITF expression in melanocytes via α-melanocyte-stimulating hormone synthesis, MC1R activation, and increase in cAMP levels. Cyclic AMP appears to control melanosome transport by two different mechanisms. The first one involves a rapid accumulation of melanosome to dendrite tips, probably through post-translational modifications that either favor Mlph interaction with actin (10) or increase Rab27A and Slp2 interaction (7). As shown in this report, the second one implies a long term effect, through the stimulation of Rab27A expression by MITF that might facilitate melanosome interaction with MLPH-Slac2a or Slp2.

In conclusion, MITF controls melanin synthesis through the regulation of tyrosinase, Tyrp1, and DCT expression and melanosome maturation via the regulation of GPR143 and Silver expression. The data gathered in the present report show that MITF also controls the peripheral distribution of melanosomes to the dendrites tips by regulating Rab27A expression. Thus MITF seems to organize the transmission of the differentiation signal and coordinates the transcriptional response, ensuring proper expression of essential genes for full functional melanocyte differentiation, pigmentation process, and UV adaptive response.

REFERENCES

1. Goding, C. R. (2007) *Int. J. Biochem. Cell Biol.* **39,** 257–259
2. Barral, D. C., and Seabra, M. C. (2004) *Pigment Cell Res.* **17,** 111–118
3. Jordens, I., Westbroek, W., Marsman, M., Rocha, N., Mommaas, M., Huizing, M., Lambert, J., Naeyaert, J. M., and Neefjes, J. (2006) *Pigment

Cell Res. **19,** 412–423

4. Bahadoran, P., Aberdam, E., Mantoux, F., Busca, R., Bille, K., Yalman, N., de Saint-Basile, G., Casaroli-Marano, R., Ortonne, J. P., and Ballotti, R. (2001) *J. Cell Biol.* **152,** 843–850

5. Nagashima, K., Torii, S., Yi, Z., Igarashi, M., Okamoto, K., Takeuchi, T., and Izumi, T. (2002) *FEBS Lett.* **517,** 233–238

6. Seabra, M. C., and Coudrier, E. (2004) *Traffic* **5,** 393–399

7. Kuroda, T. S., and Fukuda, M. (2004) *Nat. Cell Biol.* **6,** 1195–1203

8. Busca, R., and Ballotti, R. (2000) *Pigment Cell Res.* **13,** 60–69

9. Garcia-Borron, J. C., Sanchez-Laorden, B. L., and Jimenez-Cervantes, C. (2005) *Pigment Cell Res.* **18,** 393–410

10. Passeron, T., Bahadoran, P., Bertolotto, C., Chiaverini, C., Busca, R., Valony, G., Bille, K., Ortonne, J. P., and Ballotti, R. (2004) *FASEB J.* **18,** 989–991

11. Gaggioli, C., Busca, R., Abbe, P., Ortonne, J. P., and Ballotti, R. (2003) *Pigment Cell Res.* **16,** 374–382

12. Bertolotto, C., Busca, R., Abbe, P., Bille, K., Aberdam, E., Ortonne, J. P., and Ballotti, R. (1998) *Mol. Cell Biol.* **18,** 694–702

13. Levy, C., Khaled, M., and Fisher, D. E. (2006) *Trends Mol. Med.* **12,** 406–414

14. Tolmachova, T., Ramalho, J. S., Anant, J. S., Schultz, R. A., Huxley, C. M., and Seabra, M. C. (1999) *Gene* (*Amst.*) **239,** 109–116

15. de la Serna, I. L., Ohkawa, Y., Higashi, C., Dutta, C., Osias, J., Kommajosyula, N., Tachibana, T., and Imbalzano, A. N. (2006) *J. Biol. Chem.* **281,** 20233–20241

16. Busca, R., Berra, E., Gaggioli, C., Khaled, M., Bille, K., Marchetti, B., Thyss, R., Fitsialos, G., Larribere, L., Bertolotto, C., Virolle, T., Barbry, P., Pouyssegur, J., Ponzio, G., and Ballotti, R. (2005) *J. Cell Biol.* **170,** 49–59

17. McGill, G. G., Horstmann, M., Widlund, H. R., Du, J., Motyckova, G., Nishimura, E. K., Lin, Y. L., Ramaswamy, S., Avery, W., Ding, H. F., Jordan, S. A., Jackson, I. J., Korsmeyer, S. J., Golub, T. R., and Fisher, D. E. (2002) *Cell* **109,** 707–718

18. Beuret, L., Flori, E., Denoyelle, C., Bille, K., Busca, R., Picardo, M., Bertolotto, C., and Ballotti, R. (2007) *J. Biol. Chem.* **282,** 14140–14147

19. McGill, G. G., Haq, R., Nishimura, E. K., and Fisher, D. E. (2006) *J. Biol. Chem.* **281,** 10365–10373

20. Hume, A. N., Ushakov, D. S., Tarafder, A. K., Ferenczi, M. A., and Seabra, M. C. (2007) *J. Cell Sci.* **120,** 3111–3122

21. Scott, G., and Zhao, Q. (2001) *J. Investig. Dermatol.* **116,** 296–304

22. Chabrillat, M. L., Wilhelm, C., Wasmeier, C., Sviderskaya, E. V., Louvard, D., and Coudrier, E. (2005) *Mol. Biol. Cell* **16,** 1640–1650

23. Chakraborty, A. K., Funasaka, Y., Araki, K., Horikawa, T., and Ichihashi, M. (2003) *Cell Tissue Res.* **314,** 381–388

24. Wilson, S. M., Yip, R., Swing, D. A., O'Sullivan, T. N., Zhang, Y., Novak, E. K., Swank, R. T., Russell, L. B., Copeland, N. G., and Jenkins, N. A. (2000) *Proc. Natl. Acad. Sci. U. S. A.* **97,** 7933–7938

25. Bahadoran, P., Busca, R., Chiaverini, C., Westbroek, W., Lambert, J., Bille, K., Valony, G., Fukuda, M., Naeyaert, J. M., Ortonne, J. P., and Ballotti, R. (2003) *J. Biol. Chem.* **278,** 11386–11392

26. Chen, Y., Samaraweera, P., Sun, T. T., Kreibich, G., and Orlow, S. J. (2002) *J. Investig. Dermatol.* **118,** 933–940

27. Carreira, S., Goodall, J., Denat, L., Rodriguez, M., Nuciforo, P., Hoek, K. S., Testori, A., Larue, L., and Goding, C. R. (2006) *Genes Dev.* **20,** 3426–3439

28. Aksan, I., and Goding, C. R. (1998) *Mol. Cell Biol.* **18,** 6930–6938

29. Du, J., Widlund, H. R., Horstmann, M. A., Ramaswamy, S., Ross, K., Huber, W. E., Nishimura, E. K., Golub, T. R., and Fisher, D. E. (2004) *Cancer Cell* **6,** 565–576

30. Carreira, S., Goodall, J., Aksan, I., La Rocca, S. A., Galibert, M. D., Denat, L., Larue, L., and Goding, C. R. (2005) *Nature* **433,** 764–769

31. Stinchcombe, J. C., Barral, D. C., Mules, E. H., Booth, S., Hume, A. N., Machesky, L. M., Seabra, M. C., and Griffiths, G. M. (2001) *J. Cell Biol.* **152,** 825–834

32. Yi, Z., Yokota, H., Torii, S., Aoki, T., Hosaka, M., Zhao, S., Takata, K., Takeuchi, T., and Izumi, T. (2002) *Mol. Cell Biol.* **22,** 1858–1867

33. Huan, C., Kelly, M. L., Steele, R., Shapira, I., Gottesman, S. R., and Roman, C. A. (2006) *Nat. Immunol.* **7,** 1082–1091

34. Chu, K., Nemoz-Gaillard, E., and Tsai, M. J. (2001) *Recent Prog. Horm. Res.* **56,** 23–46

35. Menasche, G., Fischer, A., and de Saint Basile, G. (2002) *Am. J. Hum. Genet.* **71,** 1237–1238

36. Larribere, L., Hilmi, C., Khaled, M., Gaggioli, C., Bille, K., Auberger, P., Ortonne, J. P., Ballotti, R., and Bertolotto, C. (2005) *Genes Dev.* **19,** 1980–1985

37. Bertolotto, C., Abbe, P., Hemesath, T. J., Bille, K., Fisher, D. E., Ortonne, J. P., and Ballotti, R. (1998) *J. Cell Biol.* **142,** 827–835

38. Bertolotto, C., Bille, K., Ortonne, J. P., and Ballotti, R. (1996) *J. Cell Biol.* **134,** 747–755

Microphthalmia-associated Transcription Factor Regulates *RAB27A* Gene Expression and Controls Melanosome Transport

Christine Chiaverini, Laurent Beuret, Enrica Flori, Roser Busca, Patricia Abbe, Karine Bille, Philippe Bahadoran, Jean-Paul Ortonne, Corine Bertolotto and Robert Ballotti

Access the most updated version of this article at doi: 10.1074/jbc.M800130200

Alerts:
- When this article is cited
- When a correction for this article is posted

Click here to choose from all of JBC's e-mail alerts

This article cites 38 references, 17 of which can be accessed free at
http://www.jbc.org/content/283/18/12635.full.html#ref-list-1